CHAPTER 7

IN-VIVO STUDIES

In-vivo Studies

7.1 INTRODUCTION

Animal models of liver fibrosis remain a vital experimental tool. Animal models are essential to the investigation of liver fibrosis and other fibrotic diseases because they provide the only model in which the serial sampling of tissue, which facilitates the dissection of the cell and molecular processes that underlie fibrosis, can be made. The importance of studying human models of disease cannot be overemphasized. Nevertheless, at best they can only provide a snapshot of a disease process which may develop over weeks or months. In addition, the morbidity, potential mortality, and ethical issues associated with liver biopsy in humans, significantly limits the use of biopsy material for research. Finally, it is, of course, ethically impossible to manipulate the pathogenic process of liver fibrosis experimentally in vivo in human beings. For these reasons, animal models of liver fibrosis remain a vital experimental tool.

Many experimental models of hepatic fibrosis have been described. These include those associated with toxic damage [e.g., carbon tetrachloride, diamethylnitrozamine, thioacetamide (Ala-Kokko et al., 1989; Cameron and Karunaratne, 1936; Igarashi et al., 1986; Madden et al., 1970; Morrione, 1949; Martinez-Hernandez, 1985; Nakamura et al., 1975; Rojkind and Dunn, 1979; Rubin et al., 1963; Zimmerman, 1976)], immunological damage [e.g., that mediated by heterologous serum and experimental schistosomiasis (Ballardini et al., 1983; Yokoi et al., 1988)], biliary fibrosis [e.g., common bile duct ligation (Issa et al., 2001; Tams, 1957)], and alcoholic liver disease [e.g., the baboon ethanol diet or the Tsukamoto/French model in rats (Tsukamoto et al., 1990)].

Carbon tetrachloride-induced fibrosis and cirrhosis is one of the oldest and probably the most widely used toxin-based experimental model for the induction of fibrosis. It has the advantages that it has been clearly characterized and in many respects mirrors the pattern of disease seen in human fibrosis and cirrhosis associated with toxic damage (Tsukamoto et al., 1990; Perez Tamayo, 1983). In addition, there is extensive experience with this model with respect to the characterization of histological and biochemical changes and changes associated with injury, inflammation, and fibrosis (Perez Tamayo, 1983; Maher and McGuire, 1990). Most specifically, the cellular sources of key matrix components, including collagen-1 in addition to the matrix

degrading metalloproteinases (matrix metalloproteinases [MMPs]) and their inhibitors (tissue inhibitors of metalloproteinases [TIMPs]), have been determined (Maher and McGuire, 1990; Iredale et al., 1996; Iredale et al., 1998). Finally, in experienced hands, and even with outbreed rats or mice, this model elicits a reproducible and predictable fibrotic response, making it a valuable basis for study. For these reasons, there is a relatively extensive experience and growing literature in which CCl_4-induced fibrosis is used as a basis for mechanistic study, either through the use of genetically modified mice (Issa et al., 2003) or the manipulation of the process via a drug or other mediator (Ala-Kokko et al., 1989; Nakamura et al., 1975; Yokoi et al., 1988; Wright et al., 2001).

Of course, the CCl_4 model has disadvantages. In comparison, as a model, it has no direct human disease counterpart (Perez Tamayo, 1983). Additionally, unlike human liver fibrosis, there is more pronounced cholangiolar cell hyperplasia in advanced CCl_4 fibrosis and, in rats, in the presence of CCl_4-induced cirrhosis, and there is failure to progress to the development of hepatocellular carcinoma (this has been reported in mice subjected to CCl_4 injury, however) (Perez Tamayo, 1983). A final consideration is that, in comparison with studies of human tissue and murine tissue, the availability of protein-based reagents such as antibodies, which work effectively in rat models, is relatively limited. These comments notwithstanding, this article will describe the methods for using CCl_4 as an in vivo model of fibrosis in rats.

Carbon tetrachloride, like other halokanes, is activated by oxidases to yield a trichloromethyl radical. This free radical initiates lipid peroxidation and can react with the sulphydrol group of proteins. CCl_4 has been administered to rodents by inhalation, gastric gavage, and by subcutaneous and intraperitoneal injections. Because of the necessity for bioactivation, the severity of CCl_4 injury will be strongly influenced by the type of diet and the presence of other xenobiotics. Specifically, microsomal cytochrome p450 induction significantly enhances CCl_4-mediated damage (Tsukamoto et al., 1990; Perez Tamayo, 1983). Thus, diet or drugs that activate cytochrome p450 enhance CCl4 toxicity and the speed of development of fibrosis. This evidence has been used to increase the speed of development of fibrosis via the addition of barbiturates to drinking water in conjunction with CCl_4 intoxication (Tsukamoto et al., 1990). Conversely, of course, p450 inhibitors will reduce the toxicity and fibrosis induced by CCl_4 intoxication.

In vitro diffusion studies are dependent on the instrument's hydrodynamic condition and the diffusion medium. The in vivo parameters that help in assessing the rate and extent of absorption, AUC, Cmax and Tmax may not be sufficient to evaluate the pharmacokinetic performance, particularly the diffusion rate of controlled release liposomal formulations. However, when in vivo and in vitro data are combined it would add another useful dimension for the evaluation of a product's performance (Mojaverian et al., 1997).

Researchers have used CCl_4 experiments in a series of experimental models of liver injury and fibrosis. These include using CCl_4: to induce acute injury characterized by self-limiting hepatic stellate cell (HSC) activation and hepatocellular regeneration (Oakley et al., 2003), to develop early and established fibrosis [4–6 wk of CCl_4, administered as described later (Iredale et al., 1996; Iredale et al., 1998)], to develop early reversible cirrhosis (8 wk of CCl_4 intoxication), and to develop cirrhosis that demonstrates only partial reversibility (12 wk CCl_4 intoxication). In the current in vivo studies, using CCl_4 induced model of liver fibrosis, we determined the pharmacokinetic properties and the biodistribution of M6P-HSA conjugated liposomes in diseased animals.

7.2 ANIMALS

Specified pathogen free male Sprague-Dawley rats of 180 to 220 g were obtained from Torrent Research Centre (TRC), Gandhinagar, India. All experiments and protocols described in present study were approved by the Institutional Animal Ethics Committee (IAEC) of Pharmacy Department, The M.S. University of Baroda and with permission from Committee for the Purpose of Control and Supervision of Experiments on Animals (CPCSEA), Ministry of Social Justice and Empowerment, Government of India. All animals were housed in-group of 3 animals and maintained under standardized conditions (12-h light/dark cycle, 24 ± 2 °C, 35 to 60% humidity) and provided free access to pelleted CHAKKAN diet (Nav Maharashtra Oil Mills Pvt. Ltd., Pune) and purified drinking water ad libitum.

7.3 CAUTION

Carbon tetrachloride is toxic to humans by inhalation and ingestion. Preparation of carbon tetrachloride should take place in a fume hood. Injection of animals should take place, where possible, in a fume hood; although for experienced users, if a sealed

stock solution of CCl_4 is being used and only opened for filling syringes, then use in a well-ventilated room is probably acceptable. All unused solutions containing CCl_4 should be disposed of in accordance with local regulations.

7.4 CCL_4-INDUCED LIVER FIBROSIS MODEL AND EXPERIMENTAL DESIGN

Experimental liver fibrosis was developed, using an established protocol (Constandinou et al., 2005) with slight modification, that involved: intraperitoneal (i.p.) injections of 0.2 mL/100 g of the CCl_4:olive oil mixture (equal parts of CCl_4 and olive oil i.e. 1:1), twice weekly at equal intervals, for 2 week followed by 0.1 mL of the 1:1 ratio CCl_4:olive oil mixture for 8 weeks (i.e., rats received 0.1 mL/100 g of CCl_4 for 2 week followed by 0.05 mL CCl_4/100 g for rest of the duration). After 4 weeks from the first injection of CCl4, the rats were randomly divided into 9 subgroups (n=8):

Group 1 (control): Animals received standard laboratory diet and drinking water ad libitum and served as a control group.

Group 2 (CCl_4): Animals received only CCl_4 as per the standard protocol.

Group 3 (Plain M6P-HSA conjugated liposomes + CCl_4): Animals received plain M6P-HSA conjugated liposomes (equivalent to amount of liposomes required in group 5, intravenous) along with CCl_4.

Group 4 (RGZ + CCl_4): Animals received RGZ (1 mg/kg/day, intravenous) along with CCl_4.

Group 5 (RGZ loaded unconjugated liposomes + CCl_4): Animals received RGZ loaded unconjugated liposomes (equivalent to RGZ 1 mg/kg/day, intravenous) along with CCl_4.

Group 6 (RGZ loaded M6P-HSA conjugated liposomes + CCl_4): Animals received RGZ loaded M6P-HSA conjugated liposomes (equivalent to RGZ 1 mg/kg/day, intravenous) along with CCl_4.

Group 7 (CDS + CCl_4): Animals received CDS (3 mg/kg/day, intravenous) along with CCl_4.

Group 8 (CDS loaded unconjugated liposomes + CCl_4): Animals received CDS loaded unconjugated liposomes (equivalent to CDS 3 mg/kg/day, intravenous) along with CCl_4.

Group 9 (CDS loaded M6P-HSA conjugated liposomes + CCl_4): Animals received CDS loaded M6P-HSA conjugated liposomes (equivalent to CDS 3 mg/kg/day, intravenous) along with CCl_4.

All formulations were administered via the tail-vein injection.

7.5 BIOCHEMICAL ESTIMATION

After 8 weeks from the first injection of CCl_4, animals were sacrificed and blood samples were collected and serum separated from each sample and used for the biochemical analysis. Serum albumin (ALB), globulin (GLB), total protein, alanine amino-transferase (ALT), glutamate-pyruvate transaminase (AST) and blood glucose were measured by routine biochemical methods utilizing kits according to the manufacturer's instructions (described in chapter 3). Serum levels of hyaluronic acid were measured by ELISA kits according to the manufacturer's instructions (described in chapter 3). Immediately after sacrifice, liver was isolated in ice cold condition. They were blotted free of blood and tissue fluids. Then were weighed and stored at -80 °C till further use for the further analysis (CryoScientific, India). Liver weight to body weight ratio (liver coefficient) was calculated by dividing liver weight (g) by body weight (g) and multiplying it with 100 (Ye and Liu, 1985).

7.6 HYDROXYPROLINE CONTENT OF LIVER TISSUE

Hydroxyproline content of the liver tissue was determined according to Boyd R. Switzer's method as previously reported (described in chapter 3) (Switzer, 1991). The data was expressed as hydroxyproline (µg)/wet liver weight (g).

7.7 HISTOPATHOLOGY

After sacrificing the animals, liver was immediately removed and washed with saline and fixed in 10% buffered formalin. The fixed tissues were embedded in paraffin, five µm thick serial sections were cut and then processed for hematoxylin and eosin (H&E), masson's trichrome, picro-sirius red and α-SMA staining according to standard procedures (Constandinou et al., 2005).

7.7.1 Hematoxylin and Eosin Staining

Hematoxylin and eosin staining provides a specimen in which the overall architecture, degree of inflammation, necrosis, cellular apoptosis, and cellular mitosis can be assessed. For paraffin-embedded tissue sections:

1. Dip tissue sections in filtered Mayer's Haemalum for approx 30 s to 1 min.
2. Thoroughly wash tissue sections in tap water until the water is clear.
3. Blue tissue sections in Scott's tap water for 1 min.
4. Thoroughly wash tissue sections in tap water.
5. Dip tissue sections in eosin for 30 s.
6. Thoroughly wash tissue sections in tap water until the water is clear.
7. Dehydrate tissue sections through IMS twice, followed by xylene twice, each time for 5 min.
8. Sections were mounted using cover slips with distrene, plasticizer, xylene (DPX) medium.

7.7.2 Masson's Trichrome Staining

Description: This method is used for the detection of collagen fibers in tissue specimens on formalin-fixed, paraffin-embedded sections, and may be used for frozen sections as well. The collagen fibers will be stained blue and the nuclei will be stained black and the background is stained red.

Fixation: 10% formalin or Bouin's solution

Solutions and Reagents:

Bouin's Solution:

Picric acid (saturated) ---------- 75 ml

Formaldehyde (37-40%) ---------- 25 ml

Glacial acetic acid ---------- 5 ml

Mix well. This solution will improve Masson Trichrome staining quality.

Weigert's Iron Hematoxylin Solution:

Stock Solution A:

Hematoxylin ---------- 1 g

95% Alcohol ---------- 100 ml

Stock Solution B:

29% Ferric chloride in water --------- 4 ml

Distilled water ---------- 95 ml

Hydrochloric acid, concentrated ---- 1ml

Weigert's Iron Hematoxylin Working Solution:

Mix equal parts of stock solution A and B. This working solution is stable for 3 months (no good after 4 months)

Biebrich Scarlet-Acid Fuchsin Solution:

Biebrich scarlet, 1% aqueous --------- 90 ml

Acid fuchsin, 1% aqueous ----------10 ml

Acetic acid, glacial ---------- 1 ml

Phosphomolybdic-Phosphotungstic Acid Solution:

5% Phosphomolybdic acid ---------- 25 ml

5% Phosphotungstic acid ---------- 25 ml

Aniline Blue Solution:

Aniline blue ---------- 2.5 g

Acetic acide, glacial ---------- 2 ml

Distilled water ---------- 100 ml

1% Acetic Acid Solution:

Acetic acid, glacial ---------- 1 ml

Distilled water ---------- 99 ml

Procedure:

1. Deparaffinize and rehydrate through 100% alcohol, 95% alcohol 70% alcohol.
2. Wash in distilled water.
3. For Formalin fixed tissue, re-fix in Bouin's solution for 1 hour at 56 C to improve staining quality although this step is not absolutely necessary.
4. Rinse running tap water for 5-10 minutes to remove the yellow color.
5. Stain in Weigert's iron hematoxylin working solution for 10 minutes.
6. Rinse in running warm tap water for 10 minutes.
7. Wash in distilled water.
8. Stain in Biebrich scarlet-acid fuchsin solution for 10-15 minutes. Solution can be saved for future use.
9. Wash in distilled water.
10. Differentiate in phosphomolybdic-phosphotungstic acid solution for 10-15 minutes or until collagen is not red.
11. Transfer sections directly (without rinse) to aniline blue solution and stain for 5-10 minutes. Rinse briefly in distilled water and differentiate in 1% acetic acid solution for 2-5 minutes.
12. Wash in distilled water.
13. Dehydrate very quickly through 95% ethyl alcohol, absolute ethyl alcohol (these step will wipe off Biebrich scarlet-acid fuchsin staining) and clear in xylene.
14. Mount tissue sections using cover slips with DPX.

7.7.3 Sirius Red Staining

Sirius Red staining identifies the collagens in a section and provides an excellent visual index of the extent and distribution of fibrosis. The following protocol is for paraffin-embedded tissue sections.

1. Thoroughly wash all tissue sections in distilled water.
2. Place tissue sections into 0.2% phosphomolybdic acid at room temperature for 5 min.
3. Transfer tissue sections into picro-Sirius Red solution (0.1 g Sirius Red F3B in 100 mL saturated aqueous picric acid for 2 h).

4. With the exception of the GMA tissue samples, briefly wash tissue sections in 0.01% hydrochloric acid.
5. Thoroughly wash ALL tissue sections in tap water.
6. Counter stain tissue sections in filtered Mayer's Hemalum for approx 30 s to 1 min.
7. Thoroughly wash tissue sections in tap water until the water is clear.
8. Blue tissue sections in Scott's tap water for 1 min.
9. Thoroughly wash tissue sections in tap water.
10. Dehydrate tissue sections through IMS twice, followed by xylene twice, each time for 5 min.
11. Mount tissue sections using cover slips with DPX.

The sections were examined under the light microscope (Olympus BX10, Tokyo, Japan) for histopathological changes and photomicrographs (Olympus DP12 camera, Japan) were taken.

Histopathological grading was blindly executed by an independent pathologist according to the Ishak Knodell score (Goodman, 2007), which allows quantifying hepatic fibrosis in grades [0 = No fibrosis, 1 = Fibrous expansion of some portal areas, with or without short fibrous septa , 2 = Fibrous expansion of most portal areas, with or without short fibrous septa, 3 = Fibrous expansion of most portal areas with occasional portal to portal bridging, 4 = Fibrous expansion of portal areas with marked bridging (portal to portal as well as portal to central), 5 = Marked bridging (portal–portal and/or portal–central) with occasional nodules (incomplete cirrhosis) and 6 = Cirrhosis, probable or definite]

The activation of liver stellate cells indicated by the staining of α-SMA filaments is also considered as a marker for the degree of hepatic fibrosis. Paraffin-embedded serial liver sections were stained for α-SMA, using α-SMA monoclonal antibodies according to the Constandinou, Henderson, and Iredale method as previously reported (Constandinou et al., 2005).

7.7.4 α-SMA Staining

α-SMA staining will identify activated HSCs and other tissue myofibroblasts in liver sections. It provides a excellent visual index of the extent and distribution of activated HSCs in areas of liver injury and fibrosis. For paraffin-embedded tissue sections:

1. Wash all tissue section in 1X D-PBS for 5 min at room temperature.
2. Retrieval of antigens masked by crosslinkages occurring during the tissue fixation process can be accomplished by placing tissue sections in preheated 0.1% trypsin in 1X D-PBS and incubating at 37°C for 20 min.
3. Thoroughly wash all tissue sections in 1X D-PBS.
4. Endogenous peroxidase activity can be blocked by placing tissue sections into 0.6% hydrogen peroxide in methanol solution for 15 min at room temperature.
5. Thoroughly wash all tissue sections in 1X D-PBS.
6. To reduce background secondary staining, add 100 µL of normal horse blocking serum (from the VECTASTAIN Universal Quick kit) diluted 1:40 in 1X D-PBS to the tissue section and incubate at room temperature for 10 min.
7. Remove excess serum and add 100 µL of α-sma diluted 1:40 in 1X D-PBS. Incubate the tissue sections in a humidity chamber at 4°C overnight. No primary antibody and/or equivalent concentrations of mouse IgG2a can be added to tissue sections to act as negative controls. Vascular structures in the liver tissue sections or muscle tissue can act as positive controls.
8. Wash tissue sections in 1X D-PBS for 5 min.
9. Add 100 µL of biotinylated universal secondary antibody (from the VECTASTAIN Universal Quick kit) diluted 1:20 in 1X D-PBS with blocking serum diluted 1:10. Incubate the tissue sections at room temperature for 15 min.
10. Wash tissue sections in 1X D-PBS for 5 min.
11. Add 100 µL of streptavidin/peroxidase preformed complex antibody (from the VECTASTAIN Universal Quick kit) diluted 1:40 in 1X D-PBS. Incubate the tissue sections at room temperature for 10 min.
12. Wash tissue sections in 1X D-PBS for 5 min.
13. Antigen visualization can be performed adding 100 µL of DAB (from the DAB substrate kit, to 5 mL distilled water add two drops of buffer, pH 7.5; four drops of DAB; and two drops of H2O2). α-sma antigen bound substrate is converted to an insoluble brown product.
14. Wash tissue sections thoroughly in tap water.
15. Dip tissue sections in filtered Mayer's Hemalum for approx 30 s to 1 min.
16. Thoroughly wash tissue sections in tap water until the water is clear.

17. Blue tissue sections in Scott's tap water for 1 min.Thoroughly wash tissue sections in tap water.
18. Dehydrate tissue sections through IMS twice, followed by xylene twice, each time for 5 min.
19. Mount tissue sections using cover slips with DPX.

7.8 PHARMACOKINETIC AND BIODISTRIBUTION

After 8 weeks of first injection of CCl_4, rats were injected with drug loaded M6P-HSA conjugated liposomes [(equivalent to RGZ 1 mg/kg, intravenous) or (equivalent to CDS 3 mg/kg, intravenous)], drug loaded unconjugated liposomes [(equivalent to RGZ 1 mg/kg, intravenous) or (equivalent to CDS 3 mg/kg, intravenous)] and plain drug (RGZ: 1 mg/kg or CDS: 1 mg/kg). Blood samples were collected at different time intervals of 5, 10, 20, 30 min and 1 h after injection. Total amount of the drug present in serum at each time point was measured by HPLC method (described in chapter 3). Similar experiments were performed for conjugated liposomes in rats pre-injected with M6P-HSA or HSA at the dose of 13 mg/kg of body weight (intravenous) 5 min before the injection of drug loaded M6P-HSA conjugated liposomes [(equivalent to RGZ 1 mg/kg, intravenous) or (equivalent to CDS 3 mg/kg, intravenous)]. From the obtained serum concentration data, the pharmacokinetic parameters were derived for each group using the Thermo Kinetica program. (Version 5.0, Thermo Fisher Scientific).

After one hour of injection, liver, spleen, kidneys, lungs and heart were excised, made free from any adhering tissues, weighed and drug content was measured in each organ by HPLC method after extraction (described in chapter 3).

7.9 RESULTS AND DISCUSSION

7.9.1 Biochemical Estimation and Histopathological Examination

The physical parameters such as liver fibrosis grade and liver:body weight ratio (i.e. liver coefficient) were significantly increased in the CCl_4 induced liver fibrosis group rats compared to control group. Biochemical parameters such as serum AST, ALT, total bilirubin, hyaluronic acid and liver hydroxyproline were significantly increased and serum albumin/globulin ratio was significantly reduced in fibrotic rats. Plain RGZ, plain CDS, RGZ as well as CDS loaded unconjugated liposome treated groups

demonstrated very modest improvement in the physical and biochemical parameters. Blank conjugated liposomes displayed slight improvement due to presence of bioactive lipid DLPC and targeting ability. Most improvement, i.e. 13 to 70% in physical and biological parameters, had been observed in RGZ loaded conjugated liposome and CDS loaded conjugated liposome treated animal groups. Fibrosis grade, liver coefficient, serum AST, ALT, total bilirubin, hyaluronic acid and liver hydroxyproline content were significantly reduced and serum albumin/globulin ratio was increased as compared to CCl_4 induced liver fibrosis model group rats as given in the table 7.1 and 7.2. Significant reduction in serum glucose level was observed for plain RGZ and RGZ loaded unconjugated liposomes but no significant change was observed for RGZ loaded M6P-HSA conjugated liposomes suggesting very minimal or no systemic side effects of RGZ when given in conjugated liposomes.

The sections were stained with hematoxylin and eosin (H&E), mason's trichrome, picro-Sirius red and for α-SMA and then examined under the light microscope for histopathological changes and photomicrographs were taken (figure 7.1). Sections taken from rats of the control group showed normal architecture and have very less collagen and α-SMA deposition. The tissue architecture was very much disordered in the sections from fibrosis model group. Collagen and α-SMA depositions were also much more extensive. Here also the improvement was in order of RGZ loaded conjugated liposome = CDS loaded conjugated liposome > blank conjugated liposomes > RGZ loaded unconjugated liposomes = CDS loaded unconjugated liposomes > plain RGZ = plain CDS.

Figure 7.1 Representative histopathological images (I: hematoxylin and eosin, II: mason's trichrome, III: Picro-Sirius red and IV: α -smooth muscle actin staining) of liver tissues of A: Control, B: CCl_4 treated, C: Plain M6P-HSA conjugated liposomes plus CCl_4, D: Plain RGZ plus CCl_4, E: RGZ loaded unconjugated liposomes plus CCl_4, F: RGZ loaded M6P-HSA conjugated liposomes plus CCl_4, G: Plain CDS plus CCl_4, H: CDS loaded unconjugated liposomes plus CCl_4, I: CDS loaded M6P-HSA conjugated liposomes plus CCl_4. (formulations equivalent to RGZ 1 mg/kg/day or CDS 3 mg/kg/day, intravenous)

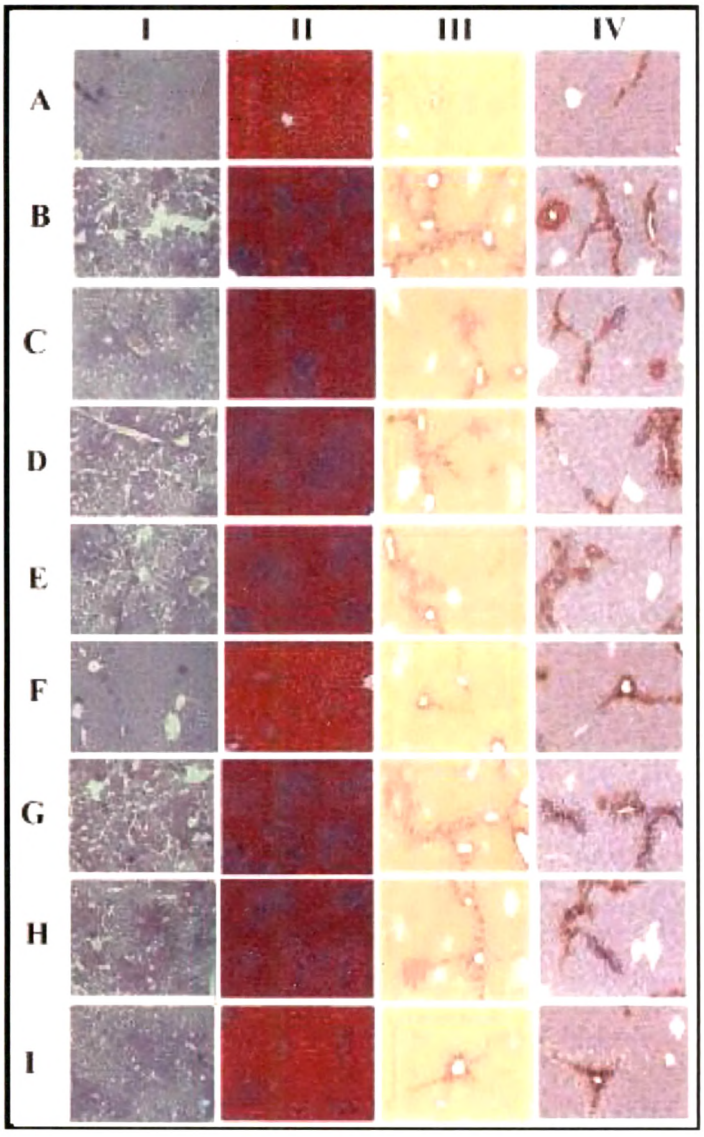

Table 7.1 The effect of various treatments on body weight, liver weight, liver coefficient and fibrosis grade

Formulation	Body weight (g)	Liver Weight (g)	Liver Coefficient	Fibrosis grade
Control	401.57 ± 19.29	14.53 ± 1.071	3.61 ± 0.101	--
CCl_4	307.67 ± 15.52	15.80 ± 1.185	5.12 ± 0.129	4.33 ± 0.110
CCl4 + Plain M6P-HSA conjugated liposomes	318.43 ± 11.33	14.90 ± 0.954	4.67 ± 0.135*	3.88 ± 0.072**
CCl4 + RGZ	317.00 ± 13.11	15.83 ± 1.041	4.99 ± 0.131	4.21 ± 0.042
CCl4 + RGZ loaded unconjugated liposomes	320.20 ± 17.07	15.47 ± 1.186	4.82 ± 0.115	4.04 ± 0.083
CCl4 + RGZ loaded M6P-HSA conjugated liposomes	328.73 ± 14.34	14.33 ± 0.984	4.35 ± 0.111***	3.17 ± 0.110***
CCl4 + CDS	312.37 ± 13.11	15.91 ± 1.182	5.09 ± 0.107	4.27 ± 0.030
CCl4 + CDS loaded unconjugated liposomes	316.81 ± 12.98	15.66 ± 0.956	4.94 ± 0.128	4.08 ± 0.042
CCl4 + CDS loaded M6P-HSA conjugated liposomes	325.19 ± 16.21	14.51 ± 1.110	4.46 ± 0.124***	3.25 ± 0.072***

n = 10 (± SEM)

* $p < 0.05$, ** $p < 0.01$, *** $p < 0.001$ vs. the CCl_4 treated group. Significance was determined by one way analysis of AVONA followed by Tukey's multiple comparison test.

Table 7.2 The effect of various treatments on serum AST, ALT, A/G ratio, total bilirubin, hyaluronic acid, glucose and liver hydroxyproline content

Formulation	ALT (IU/L)	AST (IU/L)	Serum Albumin/ Globulin ratio	Total Bilirubin (mg/dl)	Serum Hyaluronic acid (ng/ml)	Liver Hydroxyproline (µg/g)	Serum Glucose (mg/dl)
Control	31.48 ± 4.379	91.21 ± 4.859	1.89 ± 0.056	0.44 ± 0.035	46.79 ± 4.851	295.15 ± 7.695	97.31 ± 1.390
CCl_4	88.85 ± 5.544	212.60 ± 5.088	0.99 ± 0.055	2.11 ± 0.046	198.95 ± 4.016	1881.96 ± 8.704	96.18 ± 1.005
CCl4 + Plain M6P-HSA conjugated liposomes	71.00 ± 4.254 **	182.89 ± 4.853 ***	1.29 ± 0.049***	1.79 ± 0.049 ***	145.25 ± 5.722***	1730.68 ± 7.796 ***	97.24 ± 1.210
CCl4 + RGZ	81.86 ± 4.464	203.55 ± 5.115	1.06 ± 0.035	2.02 ± 0.041	187.75 ± 3.958	1855.00 ± 4.731	81.96 ± 1.200 ***
CCl4 + RGZ loaded unconjugated liposomes	78.11 ± 4.106	194.92 ± 4.462 **	1.17 ± 0.043**	1.88 ± 0.047 ***	172.78 ± 4.945***	1843.03 ± 6.078**	85.02 ± 1.258 ***
CCl4 + RGZ loaded M6P-HSA conjugated liposomes	46.69 ± 5.433 ***	128.24 ± 4.568 ***	1.69 ± 0.042***	1.18 ± 0.041 ***	88.61 ± 4.945***	1310.31 ± 5.710 ***	92.18 ± 1.156
CCl4 + CDS	85.12 ± 5.208	206.04 ± 5.115	1.07 ± 0.051	2.06 ± 0.037	188.21 ± 4.156	1867.74 ± 8.664	--
CCl4 + CDS loaded unconjugated liposomes	80.01 ± 4.663	198.23 ± 4.462*	1.13 ± 0.036	1.94 ± 0.043*	177.93 ± 3.763**	1840.63 ± 7.917**	--
CCl4 + CDS loaded M6P-HSA conjugated liposomes	56.27 ± 3.994 ***	140.07 ± 4.568 ***	1.53 ± 0.038***	1.34 ± 0.045 ***	95.53 ± 3.442***	1363.55 ± 6.638 ***	--

n = 10 (± SEM)

* $p < 0.05$, ** $p < 0.01$, *** $p < 0.001$ vs. the CCl_4 treated group (For all except Serum glucose).

* $p < 0.05$, ** $p < 0.01$, *** $p < 0.001$ vs. the control group (For serum glucose).

Significance was determined by one way analysis of AVONA followed by Tukey's multiple comparison test.

7.9.2 Pharmacokinetic and Biodistribution

After 8 weeks of first injection of CCl_4, blood clearance of plain drug, unconjugated liposomes and conjugated liposomes were compared (figure 7.2 and 7.3). After 10 min of injection, almost 87.91% of the injected dose for RGZ loaded conjugated liposomes cleared from the blood circulation, which was 2.61 folds higher than RGZ unconjugated liposomes and 4.93 folds higher than plain RGZ. After one hour, only 3.12% of the injected dose was present in the blood for RGZ loaded conjugated liposomes, which were 11.03 and 24.27 folds lower than RGZ loaded unconjugated liposomes and plain RGZ respectively.

After 10 min of injection, almost 88.27% of the injected dose for CDS loaded conjugated liposomes cleared from the blood circulation, which was 2.57 folds higher than CDS unconjugated liposomes and 5.23 folds higher than plain CDS. After one hour, only 3.53% of the injected dose was present in the blood for CDS loaded conjugated liposomes, which were 10.49 and 21.35 folds lower than CDS loaded unconjugated liposomes and plain CDS respectively.

Prior injection of M6P-HSA significantly reduced the blood clearance and increased half life of RGZ loaded and CDS loaded conjugated liposomes (table 7.3).

Figure 7.2 Pharmacokinetic profiles of RGZ (different formulations) after single intravenous bolus injection in fibrotic rats. The data represent the mean ± SEM (n = 6)

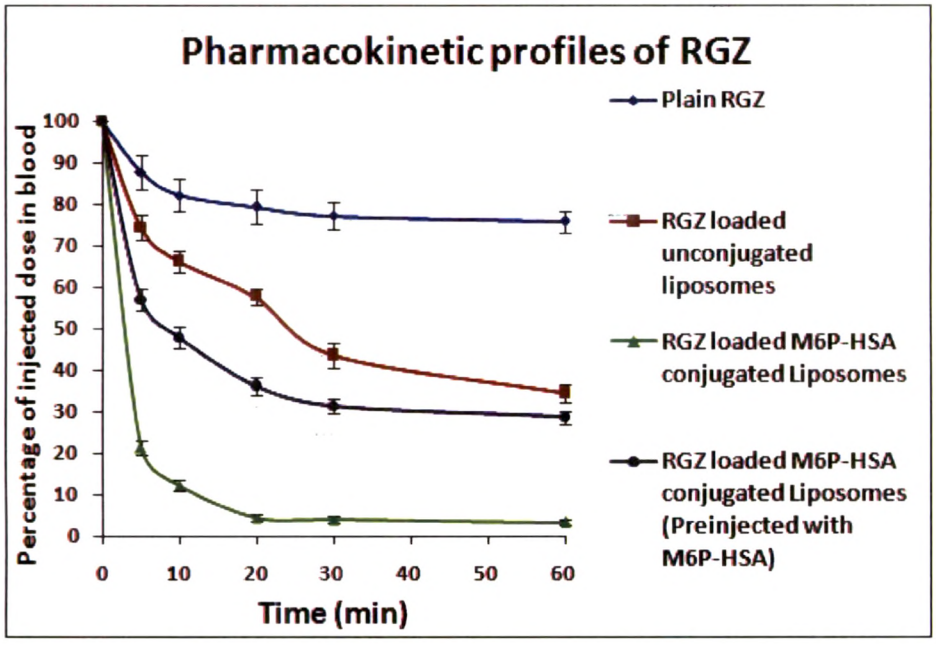

Figure 7.3 Pharmacokinetic profiles of CDS (different formulations) after single intravenous bolus injection in fibrotic rats. The data represent the mean ± SEM (n = 6)

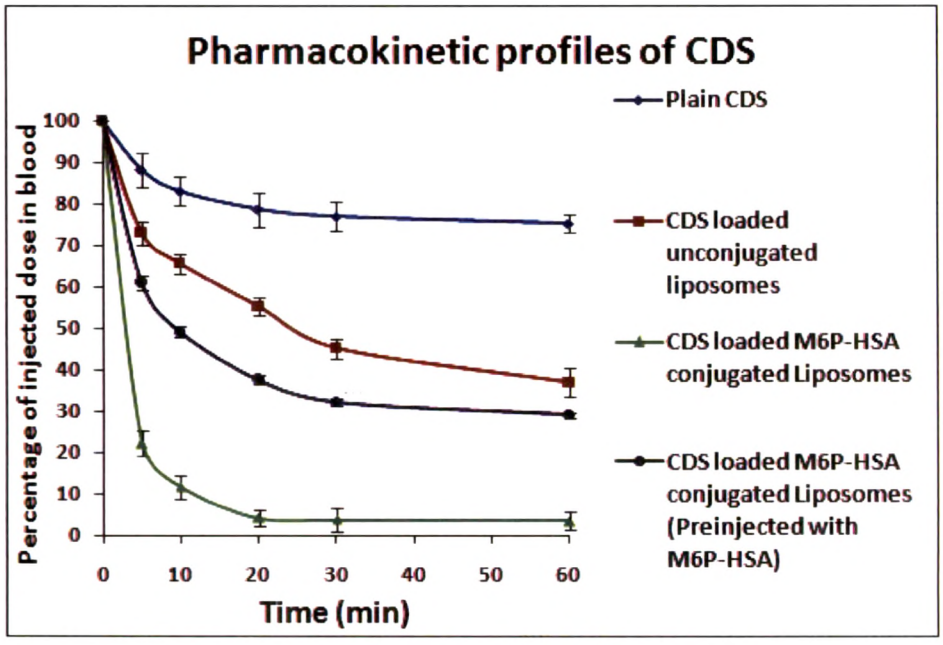

Table 7.3 The pharmacokinetic parameters for different formulations in fibrotic rats after single intravenous bolus injection. The data represent the mean ± SEM (n = 6)

Formulation	AUC (µg·min/ml)	MRT (min)	$T_{1/2}$ (min)	K_{el} (min^{-1})	V (ml)	CL (ml/min)
Plain RGZ	3653.14 ± 28.73	281.48 ± 5.11	195.11 ± 6.61	0.0036 ± 0.0003	23.66 ± 1.63	0.084 ± 0.004
RGZ loaded unconjugated liposomes	724.72 ± 10.91	60.98 ± 3.27	42.27 ± 4.56	0.0164 ± 0.0013	25.83 ± 2.05	0.424 ± 0.032
RGZ loaded M6P-HSA conjugated liposomes	51.66 ± 3.39	27.62 ± 2.93	19.15 ± 1.28	0.0362 ± 0.0025	164.13 ± 8.83	5.942 ± 0.921
RGZ loaded M6P-HSA conjugated liposomes (Pre-injected with M6P-HSA)	522.74 ± 7.84	60.54 ± 4.17	41.96 ± 3.89	0.0165 ± 0.0016	35.56 ± 2.76	0.587 ± 0.044
Plain CDS	3193.47 ± 24.58	302.27 ± 4.72	201.34 ± 4.63	0.0039 ± 0.0002	24.75 ± 1.49	0.087 ± 0.006
CDS loaded unconjugated liposomes	633.53 ± 11.08	62.12 ± 2.18	43.71 ± 2.24	0.0168 ± 0.0011	26.97 ± 1.83	0.438 ± 0.028
CDS loaded M6P-HSA conjugated liposomes	45.16 ± 2.52	25.86 ± 2.73	18.21 ± 1.77	0.0348 ± 0.0031	168.46 ± 6.18	5.876 ± 1.035
CDS loaded M6P-HSA conjugated liposomes (Pre-injected with M6P-HSA)	456.96 ± 5.94	58.91 ± 3.19	41.18 ± 2.58	0.0164 ± 0.0013	34.19 ± 1.97	0.528 ± 0.036

After one hour of injection, liver, spleen, kidneys, lungs and heart were excised and the distribution of various formulations was determined (figure 7.4 and 7.5). Almost 74.23 ± 1.55% of the injected dose had been taken up by the liver for the RGZ loaded conjugated liposomes which was 1.94 and 12.60 folds higher than RGZ loaded unconjugated liposomes and plain RGZ respectively. Very minuscule that is 4.82 ± 0.69%, 1.94 ± 0.47%, 3.61 ± 0.61% and 0.94 ± 0.2% of the injected dose had been taken up by the spleen, kidneys, lungs and heart respectively for the RGZ loaded conjugated liposomes. Amount taken up by the spleen, kidneys, lungs and heart was 2.08, 1.46, 1.08 and 1.18 folds more for RGZ loaded unconjugated liposomes and 1.10, 1.55, 0.56 and 1.43 folds more for plain drug than RGZ loaded conjugated liposomes.

Almost 73.97 ± 1.67% of the injected dose had been taken up by the liver for the CDS loaded conjugated liposomes which was 2.05 and 12.23 folds higher than CDS loaded

unconjugated liposomes and plain CDS respectively. Very minuscule that is 4.94 ± 0.71%, 1.76 ± 0.43%, 3.57 ± 0.60% and 0.91 ± 0.19% of the injected dose had been taken up by the spleen, kidneys, lungs and heart respectively for the CDS loaded conjugated liposomes. Amount taken up by the spleen, kidneys, lungs and heart was 2.00, 1.44, 1.11 and 1.29 folds more for CDS loaded unconjugated liposomes and 1.07, 1.84, 0.61 and 1.34 folds more for plain drug than CDS loaded conjugated liposomes.

Prior injection of M6P-HSA significantly reduced accumulation of RGZ and CDS in liver that is 1.60 and 1.61 folds lower than RGZ loaded conjugated liposomes and CDS loaded conjugated liposomes respectively.

Figure 7.4 Complete tissue distribution of RGZ formulations after single intravenous bolus injection. Each point represents the mean ± SEM (n=6)

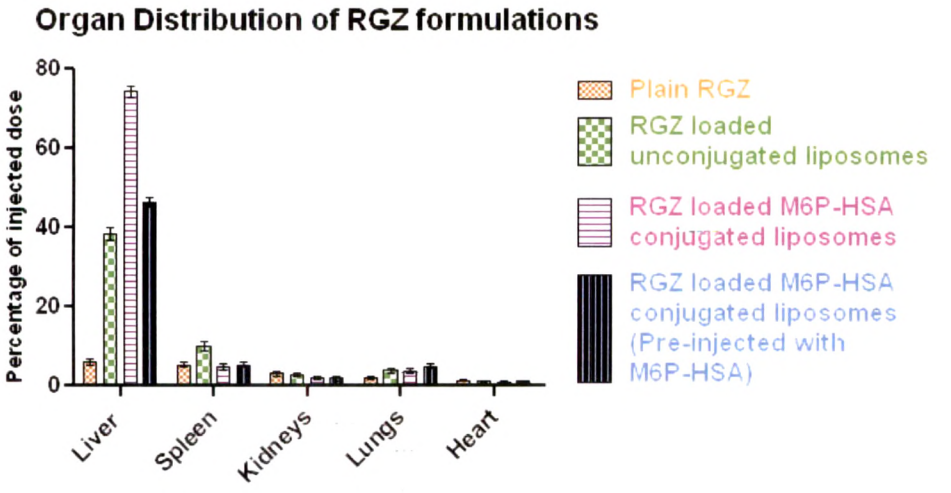

Figure 7.5 Complete tissue distribution of CDS formulations after single intravenous bolus injection. Each point represents the mean ± SEM (n=6)

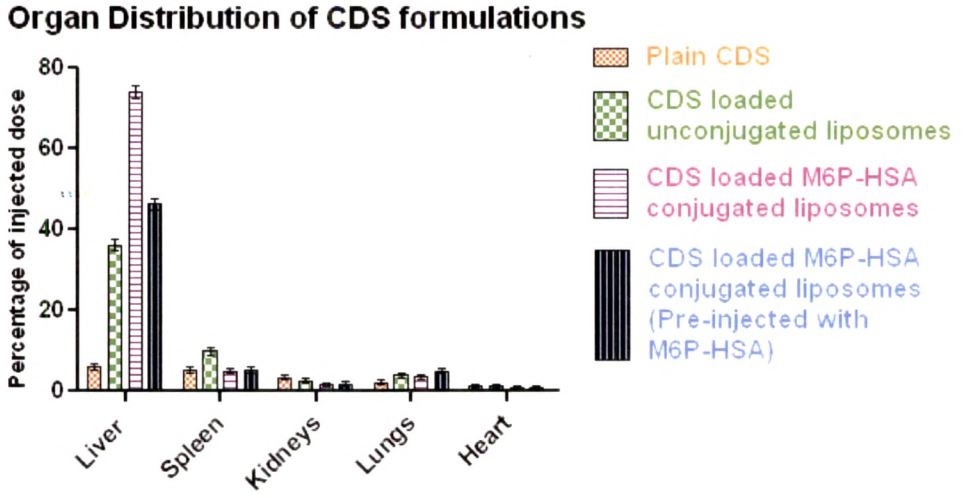

7.10 CONCLUSION

Due to lake of targeting knack plain drug and drug loaded unconjugated liposome treated groups demonstrated very modest improvement in the physical and biochemical parameters. Blank conjugated liposomes displayed slight improvement due to presence of bioactive lipid DLPC and targeting ability. Most improvement had been observed in RGZ loaded conjugated liposome and CDS loaded conjugated liposome treated animal groups. Serum glucose level estimation studied suggests very minimal or no systemic side effects of RGZ when given in conjugated liposomes.

The histopathological studies suggests that improvement was in order of RGZ loaded conjugated liposome = CDS loaded conjugated liposome > blank conjugated liposomes > RGZ loaded unconjugated liposomes = CDS loaded unconjugated liposomes > plain RGZ = plain CDS.

M6P-HSA conjugated liposomes were rapidly taken up by the target cells as compared to unconjugated liposomes and plain drug. Prior injection of M6P-HSA significantly reduced the blood clearance and increased half life of RGZ loaded and CDS loaded conjugated liposomes, which confirms target specificity of M6P-HSA conjugated liposomes.

After one hour of injection, in case of M6P-HSA conjugated liposomes, much higher percentage of injected dose had been taken up by liver as compared to unconjugated liposomes and plain drug. In comparison to unconjugated liposomes and plain drug, very minuscule percentage of the injected dose had been taken up by the spleen, kidneys, lungs and heart for the RGZ loaded conjugated liposomes. Prior injection of M6P-HSA significantly reduced accumulation of RGZ and CDS in liver which confirms target specificity of M6P-HSA conjugated liposomes.

7.11 REFERENCES

Ala-Kokko L, Stenbäck F, Ryhanen L. Preventive effect of malotilate on dimethylnitrosamine-induced liver fibrosis in the rat. J Lab Clin Med. 1989 Feb;113(2):177-83.

Ballardini G, Degli Esposti S, Bianchi FB, de Giorgi LB, Faccani A, Biolchini L, Busachi CA, Pisi E. Correlation between Ito cells and fibrogenesis in an experimental model of hepatic fibrosis. A sequential stereological study. Liver. 1983 Feb;3(1):58-63.

Cameron GR, Karunaratne WAE. Carbon tetrachloride cirrhosis in relation to liver regeneration. The Journal of Pathology and Bacteriology. 1936;42(1):1-21.

Constandinou C, Henderson N, Iredale JP. Modeling liver fibrosis in rodents. Methods Mol Med. 2005;117:237-50.

Goodman ZD. Grading and staging systems for inflammation and fibrosis in chronic liver diseases. J Hepatol. 2007 Oct;47(4):598-607.

Igarashi S, Hatahara T, Nagai Y, Hori H, Sakakibara K, Katoh M, Sakai A, Sugimoto T. Anti-fibrotic effect of malotilate on liver fibrosis induced by carbon tetrachloride in rats. Jpn J Exp Med. 1986 Oct;56(5):235-45.

Iredale JP, Benyon RC, Arthur MJ, Ferris WF, Alcolado R, Winwood PJ, Clark N, Murphy G. Tissue inhibitor of metalloproteinase-1 messenger RNA expression is enhanced relative to interstitial collagenase messenger RNA in experimental liver injury and fibrosis. Hepatology. 1996 Jul;24(1):176-84.

Iredale JP, Benyon RC, Pickering J, McCullen M, Northrop M, Pawley S, Hovell C, Arthur MJ. Mechanisms of spontaneous resolution of rat liver fibrosis. Hepatic stellate cell apoptosis and reduced hepatic expression of metalloproteinase inhibitors. J Clin Invest. 1998 Aug 1;102(3):538-49.

Issa R, Williams E, Trim N, Kendall T, Arthur MJ, Reichen J, Benyon RC, Iredale JP. Apoptosis of hepatic stellate cells: involvement in resolution of biliary fibrosis and regulation by soluble growth factors. Gut. 2001 Apr;48(4):548-57.

Issa R, Zhou X, Trim N, Millward-Sadler H, Krane S, Benyon C, Iredale J. Mutation in collagen-1 that confers resistance to the action of collagenase results in failure of

recovery from CCl4-induced liver fibrosis, persistence of activated hepatic stellate cells, and diminished hepatocyte regeneration. FASEB J. 2003 Jan;17(1):47-9.

Madden JW, Gertman PM, Peacock EE Jr. Dimethylnitrosamine-induced hepatic cirrhosis: a new canine model of an ancient human disease. Surgery. 1970 Jul;68(1):260-7; discussion 267-8.

Maher JJ, McGuire RF. Extracellular matrix gene expression increases preferentially in rat lipocytes and sinusoidal endothelial cells during hepatic fibrosis in vivo. J Clin Invest. 1990 Nov;86(5):1641-8.

Martinez-Hernandez A. The hepatic extracellular matrix. II. Electron immunohistochemical studies in rats with CCl4-induced cirrhosis. Lab Invest. 1985 Aug;53(2):166-86.

Mojaverian P, Rosen J, Vadino WA, Liebowitz S, Radwanski E. In-vivo/in-vitro correlation of four extended release formulations of pseudoephedrine sulfate. J Pharm Biomed Anal. 1997 Jan;15(4):439-45.

Morrione TG. Factors influencing collagen content in experimental cirrhosis. Am J Pathol. 1949 Mar;25(2):273-85.

Nakamura N, Fusamoto H, Koizumi T. The effects of aminoacetonitrile and its derivative on components of hepatic connective tissue in rats with chronic hepatic injury. Acta Hepatogastroenterol (Stuttg). 1975 Apr;22(2):78-84.

Oakley F, Trim N, Constandinou CM, Ye W, Gray AM, Frantz G, Hillan K, Kendall T, Benyon RC, Mann DA, Iredale JP. Hepatocytes express nerve growth factor during liver injury: evidence for paracrine regulation of hepatic stellate cell apoptosis. Am J Pathol. 2003 Nov;163(5):1849-58.

Perez Tamayo R. Is cirrhosis of the liver experimentally produced by CCl4 and adequate model of human cirrhosis? Hepatology. 1983 Jan-Feb;3(1):112-20.

Rojkind M, Dunn MA. Hepatic fibrosis. Gastroenterology. 1979 Apr;76(4):849-63.

Rubin E, Hutterer F, Popper H. Cell proliferation and fiber formation in chronic carbon tetrachloride intoxication. A morphologic and chemical study. Am J Pathol. 1963 Jun;42:715-28.

Switzer BR. Determination of hydroxyproline in tissue. J. Nutr. Biochem. 1991;2:229-31.

Symeonidis A, Trams EG. Morphologic and functional changes in the livers of rats after ligation or excision of the common bile duct. Am J Pathol. 1957 Jan-Feb;33(1):13-27.

Tams EG. Morphological and functional changes in the livers of rats after ligation and excision of the common bile duct. Am J Pathol. 1957;33:13-27.

Tsukamoto H, Matsuoka M, French SW. Experimental models of hepatic fibrosis: a review. Semin Liver Dis. 1990 Feb;10(1):56-65.

Wright MC, Issa R, Smart DE, Trim N, Murray GI, Primrose JN, Arthur MJ, Iredale JP, Mann DA. Gliotoxin stimulates the apoptosis of human and rat hepatic stellate cells and enhances the resolution of liver fibrosis in rats. Gastroenterology. 2001 Sep;121(3):685-98.

Ye ZJ, Liu YG. Effects of tetrachlorvinphos on hepatic microsomal enzymes in the rat. Acta Acad Med Wuhan. 1985;5(3):173-7.

Yokoi Y, Namihisa T, Matsuzaki K, Miyazaki A, Yamaguchi Y. Distribution of Ito cells in experimental hepatic fibrosis. Liver. 1988 Feb;8(1):48-52.

Zimmerman, H. (1976) Experimental hepatotoxicity, in Experimental Production of Disease, Part 5: Liver. (Eiciler, O., ed.), Springer-Verlag, Berlin: pp. 1–120.